Contrasting short- and long-timescale effects of vegetation dynamics on water and carbon fluxes in water-limited ecosystems

Christopher A. Williams[1] and John D. Albertson

Department of Civil and Environmental Engineering, Duke University, Durham, North Carolina, USA

Nicholas School of the Environment and Earth Sciences, Duke University, Durham, North Carolina, USA

Received 18 October 2004; revised 14 February 2005; accepted 28 February 2005; published 9 June 2005.

[1] While it is generally believed that the magnitude and composition of vegetation cover influence land-atmosphere water and carbon fluxes, observations indicate that in some cases, fluxes are insensitive to land cover contrasts. This seeming inconsistency may be resolved by contrasting fluxes over short and long timescales. To explore this potential contrast, we developed and tested a model designed to simulate daily to decadal land surface water and carbon fluxes and vegetation dynamics for water-limited ecosystems. The model reproduces ($R^2 > 0.76$) observed daily fluxes under increasing water limitation and captures representative dynamics of leaf area and fractional cover of dominant grass and wood vegetation. We parameterized the model for southern African savannas and conducted two sets of numerical experiments with either having fixed (static) grass and wood covers or allowing them to adjust dynamically with production. Static simulations reveal that the direct effect of rainfall on soil moisture is more important than the prevailing grass and wood cover states in controlling annual transpiration and production. Dynamic simulations indicate sensitivity of daily fluxes to vegetation cover states during high soil water periods. However, depletion of finite soil water prevents an integrated effect from lasting over interstorm to annual timescales. Correspondingly, while seasonal vegetation dynamics enhance seasonality in fluxes, vegetation dynamics have only minor influence on annual transpiration and production. In fact, annual rainfall explains most ($R > 0.85$) of the temporal variation in annual water and carbon fluxes. Hence, despite alteration of daily and seasonal distributions of fluxes, for water-limited ecosystems, vegetation dynamics have little effect on annual transpiration and production.

Citation: Williams, C. A., and J. D. Albertson (2005), Contrasting short- and long-timescale effects of vegetation dynamics on water and carbon fluxes in water-limited ecosystems, *Water Resour. Res.*, *41*, W06005, doi:10.1029/2004WR003750.

1. Introduction

[2] It is well established that biophysical and structural properties of vegetation can influence climate through control on land-atmosphere exchanges of momentum, mass and energy [*Charney*, 1975; *Dickinson and Henderson-Sellers*, 1988; *Soloman and Shugart*, 1993; *Neilson and Marks*, 1994; *Bonan*, 1995; *Foley et al.*, 1996; *Betts et al.*, 1997]. This broad notion is supported by numerous observational studies reporting that water or carbon fluxes differed between contrasting land covers, despite exposure to nearly identical meteorological conditions [*Joffre and Rambal*, 1993; *San Jose et al.*, 1998; *Santos et al.*, 2003; *Baldocchi et al.*, 2004; *Sakai et al.*, 2004; *von Randow et al.*, 2004]. On the contrary, some studies found that fluxes differed little between adjacent, contrasting land covers, or were insensitive to temporal variation in vegetation fractional cover [*Kabat et al.*, 1997; *Hutley et al.*, 2000; *Guillevic et al.*, 2002]. The inconsistency between these findings highlights an incomplete understanding of how temporal and spatial variation in vegetation influences land-atmosphere fluxes [e.g., *Foley et al.*, 2000; *Bonan et al.*, 2003; *Sitch et al.*, 2003].

[3] The seeming inconsistency may be resolved with closer analysis of the timescales at which fluxes respond to temporal vegetation change. *Yong-Quiang et al.* [1992] showed that increased vegetation cover initially increased daily evapotranspiration (ET, mm d^{-1}) but also caused earlier and more rapid decay of ET as soil moisture was depleted, potentially leading to little or no effect of altered vegetation cover on fluxes accumulated over a complete drying cycle. *Kabat et al.* [1997] compared ET in a semiarid woodland to that in a savanna with substantially higher vegetation cover, reporting similar total evapotranspiration over a 7-week period despite higher maximum daily evapotranspiration in the woodland. This suggests that soil water limitation prevented an accumulated effect on longer-term evapotranspiration. *Guillevic et al.* [2002] reported that in sparsely vegetated or mesic areas, monthly and annual evapotranspiration were sensitive to interannual variability in vegetation density, while markedly less sensitivity was found in densely vegetated or semiarid and arid areas, in which cases water limitation, not vegetation density, was the dominant control on accumulated water flux. Hence water limitation associated with

[1] Now at Natural Resource Ecology Laboratory, Colorado State University, Fort Collins, Colorado, USA.

0043-1397/05/2004WR003750$09.00

depletion of a finite soil water pool may prevent temporal variation in vegetation cover and composition from altering land-atmosphere water and carbon fluxes at monthly or annual timescales, even if the magnitude and temporal distribution of daily fluxes are altered.

[4] In this study, we focus on semiarid savannas because they are economically and ecologically valuable [*Eamus*, 1999] and have wide global coverage [*Atjay et al.*, 1979] and because vegetation cover and composition in semiarid areas are sensitive to climatic fluctuations [*Scholes and Archer*, 1997; *Rodriguez-Iturbe et al.*, 1999a]. Furthermore, vegetation states may influence streamflow and deep recharge to groundwater aquifers, which are relied upon for irrigation and drinking water in many dryland regions [*de Vries et al.*, 2000; *Wilcox*, 2002]. Grass, and wood (tree and shrub) vegetation types characteristic of savannas differ in their structural and physiological attributes, such as rooting depth, sensitivity to water limitation, or water use efficiency [*Scholes and Archer*, 1997]. Therefore shifts in their respective covers have the potential to alter land-atmosphere fluxes of water and carbon [*Smith et al.*, 1997].

[5] Correspondingly, some studies show that increased leaf area and vegetation cover [*Paruelo and Sala*, 1995; *Aguiar et al.*, 1996; *Jackson et al.*, 1998; *San Jose et al.*, 1998; *Baldocchi et al.*, 2004], or transition toward more deeply rooted vegetation [*Joffre and Rambal*, 1993; *Golluscio et al.*, 1998; *Ansley et al.*, 2003] can increase annual transpiration and reduce leakage. However, total fluxes over complete drying cycles, or accumulated over a growing season or year, may be insensitive to vegetation cover and composition if vegetation already accesses and consumes nearly all of the limiting soil water resource. For example, evapotranspiration in water-limited savannas typically consumes 60–100% of annual rainfall (P_a, mm yr^{-1}) [*Joffre and Rambal*, 1993; *Paruelo and Sala*, 1995; *Rodriguez-Iturbe et al.*, 1999c; *Hutley et al.*, 2001; *Laio et al.*, 2001; *Baldocchi et al.*, 2004]. Runoff, and leakage below the root zone (L, mm d^{-1}) constitute the remainder of annual rainfall, and can occur at rates faster than root water uptake, potentially making them unavoidable for certain soil types regardless of vegetation cover [*Noy-Meir*, 1973]. Hence fluxes may only be sensitive to vegetation states immediately after rain events when soil water is abundant [*Noy-Meir*, 1973; *Sala and Lauenroth*, 1982; *Sala et al.*, 1992]. As such, vegetation states may influence the temporal distribution of fluxes within a drying cycle or growing season (short timescales) but have little effect on fluxes over annual or longer timescales.

[6] Still, the partitioning of total evapotranspiration into bare soil evaporation, evaporation of intercepted rainfall, and transpiration may be responsive to vegetation states over short and long timescales [e.g., *Eagleson*, 1978b, *Rodriguez-Iturbe et al.*, 1999c; *Laio et al.*, 2001]. Transpiration, alone, has direct implications for the savanna carbon balance, since plant dry matter (DM) production (hereafter production) is directly linked to vegetation water use in savannas [*Noy-Meir*, 1973; *Verhoef et al.*, 1996; *Williams and Albertson*, 2004]. Thus the distribution of water use between competing vegetation types and their corresponding carbon fluxes (production) may exhibit long-timescale sensitivity to vegetation states.

[7] In recognition of this potential contrast between short- and long-timescale sensitivity of water and carbon fluxes to vegetation states, we address the following questions in this paper. (1) To what degree are annual surface water and carbon balances influenced by imposed static states of vegetation cover and composition in savannas? (2) How do temporal dynamics of vegetation cover and composition affect the magnitude and timing of plant water use and carbon gain in savannas?

[8] To address these two questions, we first develop a model of daily carbon and water fluxes and vegetation dynamics for mixed life form savanna communities (section 2). We verify model simulations of water and carbon fluxes at daily timescales using field data and compare simulated spatially aggregated leaf area over multi-annual timescales to remotely sensed leaf area index data (section 3.1). We then perform numerical simulations to examine the effect of different imposed static vegetation compositions on annual water and carbon fluxes under a range of rainfall conditions (section 3.2), and then relax the assumption of static vegetation to determine the role of dynamic vegetation structure and composition on fluxes in these savanna systems (section 3.3).

2. Model

[9] The model was developed to simulate temporal dynamics of the land surface water balance and vegetation carbon balance for savannas at a daily time step on a per unit ground area basis. We briefly present a conceptual overview of the model here and refer to Appendices A, B, and C and the parameters and constants in Table 1 for full model development. The land surface is divided into three fractional cover components, bare soil (f_b), grass (f_g), and wood (f_w), while leaf area index (LAI_g, LAI_w) is described within vegetated patches (Figure 1). Soil moisture in shallow (θ_1) and deep (θ_2) layers respond to inputs from precipitation (P) minus interception (I) and losses from drainage (D), bare soil evaporation (E), and grass (T_g) and wood (T_w) transpiration. Evaporation and transpiration proceed at a potential rate scaled by a widely used soil moisture limitation function. The hydrologic aspects of the model are taken mostly from *Scanlon and Albertson* [2003].

[10] We also adopt traditional formulations of vegetation growth and decay [e.g., *Chen et al.*, 1996; *LoSeen et al.*, 1997; *Calvet et al.*, 1998; *Sitch et al.*, 2003]. Plant growth is estimated from transpiration scaled by a water use efficiency (WUE) that describes the relative rates at which plants fix carbon dioxide and lose water. Net primary production (NPP) is obtained from plant growth minus respiration that is modeled with biomass, temperature, and moisture dependence. Net production is allocated to leaf or structural biomasses, also subject to decay leading to temporal dynamics of leaf areas and fractional covers. These processes are forced by daily precipitation, radiation, air temperature, and air moisture.

[11] The model is parameterized with data collected in a semiarid savanna in Ghanzi, Botswana [*Williams and Albertson*, 2004], and therefore model verification focuses on this system, but with no loss of generality in the framework and, arguably, the conclusions as they apply

Table 1. Model Parameters and Constants[a]

Parameters and Constants	Description	Typical Values	Sources[b]
$G_{s\max}$, $W_{s\max}$	maximum G_s, W_s [kg DM m^{-2} ground]	2, 4	1, 2
$LAI_{g\max}$, $LAI_{w\max}$	maximum leaf area per vegetated area [m^2 leaf m^{-2} vegetation]	2, 3	3
Γ_{gl}, Γ_{gs}, Γ_{wl}, Γ_{ws}	natural decay factor of biomass [d^{-1}]	0.0035, 0.00175, 0.0035, 0.0007	1, 4
Λ	leaf flush factor [d^{-1}]	0.05	
SLA_g, SLA_w	specific leaf area [m^2 leaf kg^{-1} DM]	10	5
α_g, α_w	ratio of intercellular to ambient CO_2 concentrations (dimensionless)	0.4, 0.6	5
$I_{g\max}$, $I_{w\max}$	maximum interception [mm d^{-1}]	1, 2	6
β_{*g}, β_{*w}	threshold for initiation of leaf flush (dimensionless)	0.7, 0.4	
ξ_{*g}, ξ_{*w}	threshold for initiation of rapid leaf turnover (dimensionless)	0.8, 0.8	
θ_{blim}, θ_{wlim}, θ_{glim}, θ_{bcr}, θ_{wcr}, θ_{gcr},	critical (*cr*) and limit (*lim*) points [m^3 H_2O m^{-3} soil]	0.05, 0.05, 0.05, 0.26, 0.12, 0.16	3, 6
ν_g, ν_w, ν_b	albedo (dimensionless)	0.24, 0.28, 0.2	6, 7
ε_1	fraction of wood roots in upper soil zone (dimensionless)	0.25	
d_1, d_2	thickness of soil zones [mm]	400, 1100	
K_{sat}	saturated hydraulic conductivity[c] [mm d^{-1}]	2000	8
ψ_e	air entry matric potential for sand [mm H_2O]	−121	8
θ_{sat}	saturated soil water content [m^3 H_2O m^{-3} soil]	0.4	8
n	soil porosity [m^3 void m^{-3} soil]	0.4	
b	soil physics parameter for sand (dimensionless)	4.05	8
Cg	soil heat flux coefficient (dimensionless)	0.3	9
ω	conversion of CO_2 exchange to dry matter [kg DM kg^{-1} CO_2]	0.55	1
C_a	ambient CO_2 concentration [μmol CO_2 mol^{-1} air]	350	
μ	parameter to clear units for WUE equation [g CO_2 g^{-1} air]	1.5×10^{-6}	
g_c, g_v	diffusivity of CO_2 or water vapor in air [m^2 s^{-1}]	2.4, 1.6	7
V	latent heat of vaporization [J kg^{-1} H_2O]	2450000	
ρ_v	density of water [Mg m^{-3}]	1	
κ	Priestley-Taylor coefficient (dimensionless)	1.26	10
γ	psychrometric constant at 100 kPa and 20°C [kPa $°C^{-1}$]	0.067	

[a]Subscripts 1, 2, *l*, *s*, *a*, *g*, *w*, *t*, and *b* refer to upper soil zone, lower soil zone, leaf, structural, annual, grass, wood, total grass plus wood, and bare soil, respectively.

[b]Sources are as follows: 1, *Scholes and Walker* [1993]; 2, *Atjay et al.* [1979]; 3, *Williams and Albertson* [2004]; 4, *Walker et al.* [1981]; 5, *Midgley et al.* [2004]; 6, *Scanlon and Albertson* [2003]; 7, *Campbell and Norman* [1998]; 8, *Clapp and Hornberger* [1978]; 9, *Lhomme and Monteny* [2000]; 10, *Brutsaert* [1982].

[c]Per unit ground area.

broadly to water-limited ecosystems. The tree-grass savanna in Ghanzi, Botswana, receives an average annual rainfall of 448 mm with an interannual standard deviation of 184 mm, based on a data set of daily rainfall collected from 1973 to 2002 at a Ghanzi weather station (D. Eaton, Daily rainfall data from 1973 to 2002 near Ghanzi, Botswana, unpublished data, 2002). Nearly all (92%) of the annual rainfall is delivered during the single, October through March growing season, unlike the bimodal distribution of annual rainfall reported for some other savannas. Table 2 presents fractional cover, leaf area, canopy height, and plant species for the dominant wood and grass vegetation common to Ghanzi. Soils are composed of coarse sand [*Baillieul*, 1975], with rapid percolation and drainage following rainfall.

[12] Several grass and wood attributes differentiated in the model characterize how vegetation states could influence water and carbon fluxes. As reported by *Williams and Albertson* [2004], the critical soil water at which transpiration departs from its potential rate is greater for grass than wood, consistent with results of *Scholes and Walker* [1993] and *Rodriguez-Iturbe et al.* [1999b], such that grass experiences more frequent and intense soil water limitation. Grass maintains a lower ratio of intercellular to ambient CO_2 concentrations owing to a more efficient photosynthetic pathway for grass (C4 rather than C3) and leading to greater grass WUE [*Walter*, 1971; *Pearcy and Ehleringer*, 1984; *Ehleringer and Monson*, 1993; *Scholes and Walker*, 1993]. Wood roots extend deeper than grass roots in many semiarid and arid ecosystems [e.g., *Schenk and Jackson*, 2002], represented with the conventional modeling approach of giving wood exclusive access to a deep soil moisture reservoir (Figure 1). Grass

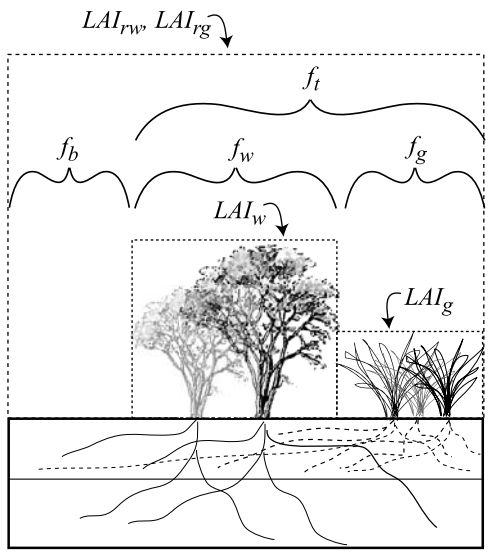

Figure 1. Schematic diagram of patch-based leaf area (LAI_x, m^2 leaf m^{-2} vegetation), ground-based leaf area (LAI_{rx}, m^2 leaf m^{-2} ground), and fractional cover (f_x, m^2 vegetation m^{-2} ground) assignments in the model.

Table 2. Range of Vegetation Fractional Cover From 136 Observations in 10 × 10 m Plots, Leaf Area Per Plant Area (LAI) Mean Canopy Heights (h), and Common Species for Wood and Grass Vegetation Types at the Ghanzi Savanna[a]

Vegetation	f_x	LAI_x[b]	h, m	Species
Wood	0.05 to 0.2	2 (4)	2.7	*Acacia erioloba, A. mellifera, A. luederitzii*, *Bauhinia* spp. *Grewia* spp., *Combretum* spp. and *Terminalia sericea*
Grass	0.6 to 0.8	1.1 (2)	0.7	*Digitaria eriantha*, *Eragrostis pallens*, *E. rigidior*, *Panicum maximum*, *Pogonarthria squarrosa*, *Setaria sphacelata*, *Stipagrostis uniplumis*, *Urochloa trichopus*

[a]From *Williams and Albertson* [2004].
[b]Maximum value is in parentheses.

supports greater fractional cover per unit of biomass [*Atjay et al.*, 1979; *Scholes and Walker*, 1993]. Finally, grass biomass decays more rapidly [*Bonan et al.*, 2003; *Sitch et al.*, 2003].

3. Results and Discussion

3.1. Model Verification

[13] Measurements of ET and canopy-scale CO_2 exchange (F_c, g CO_2 m^{-2} d^{-1}) at the Ghanzi savanna were used to evaluate the model's ability to capture daily fluxes. The field campaign, described by *Williams and Albertson* [2004], began 3 days after a large rain event (85 mm) followed by a month free of additional rain (hereafter called the dry down). The model was forced with observed meteorology. Figure 2 shows that ET and F_c were captured well, with slightly better agreement for ET (R^2 = 0.87, root-mean-squared error (rmse) = 0.27 mm d^{-1}) than for F_c (R^2 = 0.77 and rmse = 1.5 g m^{-2} d^{-1}). Slight overestimation of the magnitude of the net carbon flux when soil water and light were abundant (Figure 2, DOY 69 and 73) suggests that production was limited by other factors, possibly nutrients, during these conditions. Nonetheless, the model reproduces well the fluxes integrated over the dry down (measured and modeled ET of 51 and 52 mm and F_c of −204 and −227 g CO_2 m^{-2}), and captures the major structure of daily fluxes under increasing limitation by soil water. Since the prevailing state is one of water limitation [*Veenendaal et al.*, 2004; *Williams and Albertson*, 2004], the model is expected to provide a reasonable representation of fluxes at the daily timescale in the central Kalahari.

[14] To assess the model's ability to capture seasonal vegetation dynamics we performed a 30-year simulation forced with a stochastically generated weather series conditioned by the Eaton rainfall data set. We compared the average of daily leaf area index (LAI_{rt}, see Appendix A) for each month of the year, denoted $\langle LAI_{rt} \rangle$, to a monthly leaf area index product derived from 8 × 8 km resolution normalized difference vegetation index (NDVI) observed with advanced very high resolution radiometer (AVHRR) from 1982 to 2000 [*Myneni et al.*, 1997]. Averaging over the 18-year period to obtain the multiyear average of monthly $\langle LAI_{rt} \rangle$, denoted $\langle \langle LAI_{rt} \rangle \rangle$, the model indicates skill at the seasonal timescale with general agreement for the mean amplitude and phase (Figure 3). Despite the omission of grazing and fire effects from the model, and potential mismatch of actual and synthetically generated meteorological conditions, satellite and modeled $\langle LAI_{rt} \rangle$ are reasonably well correlated (R = 0.7). General correspondence of seasonal trends in satellite and modeled leaf area index indicates that the simple model captures representative dynamics of leaf area and vegetation cover in water-limited savannas.

3.2. Static Vegetation States and Annual Water and Carbon Fluxes

[15] We explored how the surface water balance is altered by the magnitude of imposed static states of vegetation cover for dry, average, and wet conditions. Selecting annual weather time series representative for each wetness condition (P_a = 207 mm, 413 mm, 931 mm, respectively), we repeated each series for four consecutive years, for seven static states of $\{f_g, f_w\}$, respectively, at ({0.1, 0}, {0.2, 0.05}, {0.3, 0.1}, {0.4, 0.15}, {0.5, 0.2}, {0.6, 0.25}, {0.7, 0.3}). For static simulations throughout the paper, we assumed LAI_g = 1 and LAI_w = 1 (referring to leaf areas within vegetated fractions as in Figure 1).

[16] Figure 4 shows the fraction of annual rainfall consumed by each of the surface water losses, including transpiration, bare soil evaporation, direct evaporation of interception storage, and leakage, as a function of vegetation cover. We present results from only the fourth simula-

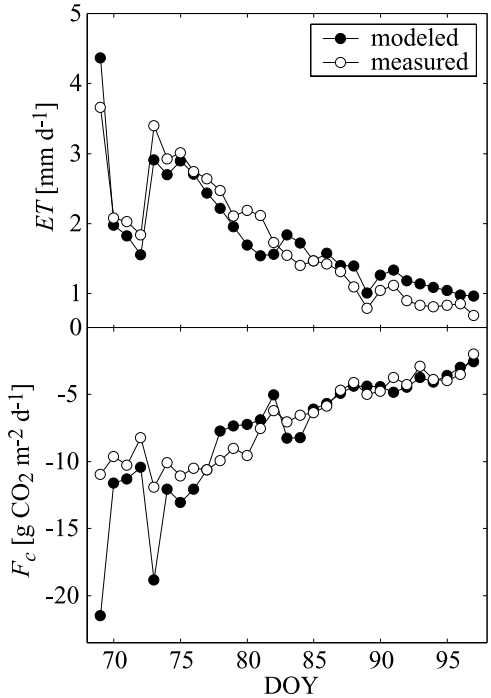

Figure 2. Measured and modeled ET and F_c for a month-long dry down experiment in Ghanzi, Botswana. Measurements are from *Williams and Albertson* [2004].

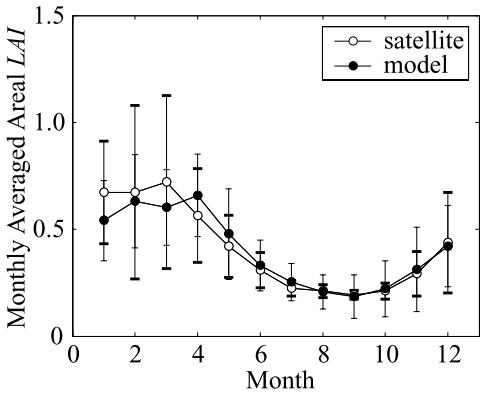

Figure 3. Satellite-derived and modeled leaf area index, shown as the annual average of leaf area index averaged for each month of the year ($\langle\langle \mathrm{LAI}_{rt} \rangle\rangle$, circles) for 1982 to 2000, with bars indicating ±1 standard deviation, where thick bars correspond to the satellite data.

tion year to diminish effects of initial soil moisture. For the range of vegetation cover typical of the central Kalahari growing season (0.4 to 0.9) [*Scholes et al.*, 2002; *Caylor et al.*, 2003], transpiration consumes a relatively constant fraction (∼0.8) of annual rainfall in simulations with dry and average conditions, and increases nearly linearly with total vegetation cover for the wet condition (Figure 4). The sum of evaporative fluxes is nearly independent of total vegetation cover over its full range, consuming nearly all of annual rainfall except in the wettest condition when leakage consumes a significant fraction. These results are consistent with tracer studies and groundwater modeling for the central Kalahari, which revealed leakage of 0 to 5 mm y^{-1} for sites with annual rainfall of 200 to 400 mm y^{-1} [*de Vries et al.*, 2000]. Our findings are also consistent with *Eagleson's* [1978a] analytical analysis, as well as numerical hydrology models applied to the semiarid regions of the Patagonian steppe [*Paruelo and Sala*, 1995] and a Mediterranean region of Spain [*Bellot et al.*, 2001] that report an approximately exponential response of leakage to annual rainfall above a threshold annual rainfall. In summary, annual evapotranspiration and leakage are largely insensitive to the magnitude of imposed static states of vegetation cover typical of the central Kalahari, except in the wettest years when water limitation is relatively low.

[17] To explore the effect of vegetation composition on the annual water balance, we performed additional simulations for static grass and wood covers ranging between 0 and 1 in increments of 0.1 and including all possible combinations of these incremental f_g and f_w states that satisfy $f_t \leq 1$, yielding 66 simulations. Each simulation was forced with the 30-year weather series used in section 3.1. Figure 5 shows the fraction of annual rainfall consumed by each of the surface water losses averaged over the 30 simulation years for three representative states of total vegetation cover. The sum of evaporative fluxes is nearly independent of vegetation composition, except near complete grass cover (i.e., $f_g/f_t \rightarrow 1$). As the static state f_w approaches zero, leakage increases and total transpiration decreases, suggesting that wood transpiration consumes a portion of annual rainfall that is not available to the shallow grass root system and is lost to leakage in the absence of wood fractional cover. Sensitivity of leakage to the presence of wood is consistent with the work of *Joffre and Rambal* [1993], who reported higher leakage and runoff in herbaceous-only as compared treed areas in oak savannas of the southwestern Iberian Peninsula. Similarly, *Gaze et al.* [1998] reported that clearing of shrubs in a tropical savanna would increase leakage by reducing dry season evapotranspiration that would otherwise be sustained by water uptake from deep roots. Still, our findings indicate that water fluxes at the annual timescale are largely insensitive to vegetation states over their typical ranges.

[18] Unlike the annual surface water balance, the annual carbon balance is sensitive to both the magnitude and composition of vegetation cover for a wide range of wood and grass cover states (Figure 6). Except at very low vegetation cover ($f_t = 0.2$), total annual net primary production generally increases with increased vegetation cover. However, the gain diminishes as production becomes increasingly limited by water availability. Furthermore, even though total annual transpiration is insensitive to relative grass cover (Figure 5), total annual net primary production generally increases with relative grass cover (Figure 6). This is associated with lower biomass per unit of plant cover for grass than wood, and hence less respiration per unit of cover for grass. The slight decrease in net primary production with

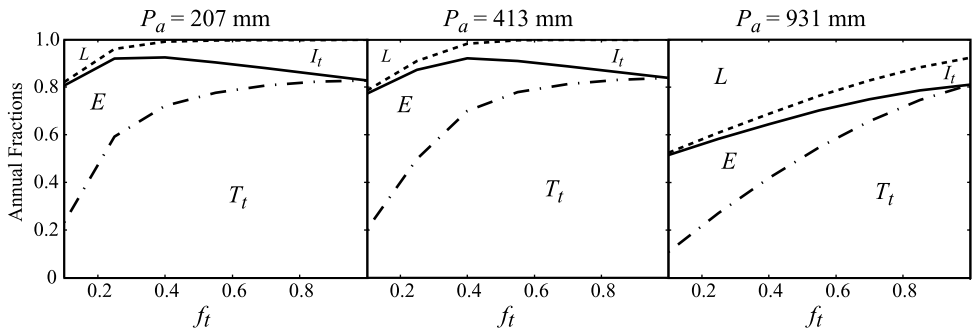

Figure 4. Fractions of annual rainfall consumed by the surface water losses obtained by dividing each loss by annual precipitation (P_a) versus vegetation fractional cover (f_t), where the dash-dotted line is total grass plus wood transpiration (T_t), the solid line is transpiration plus bare soil evaporation ($T_t + E$), and the dashed line is transpiration plus soil evaporation plus interception from grass plus wood ($T_t + E + I_t$), leaving the fraction above the dashed line to leakage (L), for dry, intermediate, and wet conditions.

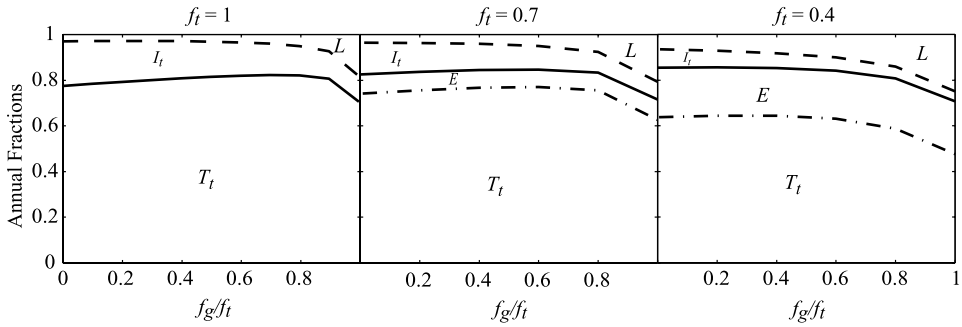

Figure 5. Annual fractions of the surface water losses (as in Figure 4) versus the grass fraction of total vegetation fractional cover (f_g/f_t) for three states of total vegetation cover (f_t).

increased relative grass cover from ~0.9 to 1.0 is consistent with a similar decrease in total transpiration, again, indicating that a minimum wood cover is required for full exploitation of the water available in the shallow and deep root compartments. Overall, static simulations indicate that annual carbon exchange is sensitive to the imposed static states of grass and wood vegetation.

[19] Rather than studying aggregate land surface fluxes, we now examine how vegetation cover and composition alter individual (grass and wood) fluxes, central to changes in vegetation states over time and associated competitive interactions. Using results from the same 66 simulations described above, we study how annual grass and wood transpiration and annual grass and wood net primary production are influenced by the magnitude of cover for each vegetation type. For simplicity, we only present results for cases with competitor cover of 0 and 0.5.

[20] Wood acquires a larger fraction of annual rainfall than grass does for the same vegetation cover (Figure 7a) owing to woods exclusive access to deep soil moisture. Responses of grass and wood annual transpiration to increased vegetation cover exhibit asymptotic behavior. This behavior is associated with a negative feedback between transpiration and soil moisture combined with finite rainfall, despite the instantaneous linear relationship between transpiration and vegetation cover (see equation (A6)). Hence temporal fluctuations in vegetation cover are expected to have little lasting (long timescale) influence on total transpiration due to water limitation, unless low total vegetation cover prevents vegetation from rapidly exhausting the water resource and leads to increased leakage. Even though wood transpires more water for the same fractional cover, grass is more productive (Figure 7c) owing to less respiration per unit of vegetation cover and higher WUE for grass. Thus changes in vegetation composition may influence total annual production and hence carbon fluxes even if total annual water use is affected little. Since static cover simulations reveal that water limitation is more important than vegetation structure in controlling annual transpiration and production, it is likely that the direct effects of seasonal and interannual dynamics of rainfall exert greater control than vegetation dynamics on total annual transpiration and net primary production, as examined in the following section.

[21] These findings have potential implications for assessing grass and wood competitive interactions. Correspondingly, competition is an important mechanism governing vegetation change (dynamics). Thus we briefly explore what our results imply about the nature of grass-wood competitive interactions. Even though wood acquires more water per unit of cover, competition for soil water is symmetric for a wide range of cover, as the same increase in competitor cover causes similar reductions in annual transpiration for grass and wood (Figure 7b). In contrast, the effect of competition on plant production is asymmetric, as competition causes a larger absolute reduction in grass production (Figure 7d). This suggests that grass exploits the production inefficiency of trees, while being dominated (and disproportionately suppressed) in terms of total production. These results are consistent with the notion that water limitation prevents competitive exclusion of grass despite wood dominance [*Scholes and Archer*, 1997; *House et al.*, 2003].

3.3. Influence of Vegetation Dynamics on Water and Carbon Fluxes

[22] Up to this point, we have used static vegetation simulations to assess how annual savanna water and carbon fluxes are altered by prevailing vegetation states. We now examine how temporal dynamics of grass and wood cover influence the magnitude and timing of transpiration and production. To this end, we contrast the dynamic simulation described in section 3.1, to a new static simulation, where f_g and f_w were fixed at the mean growing season (October

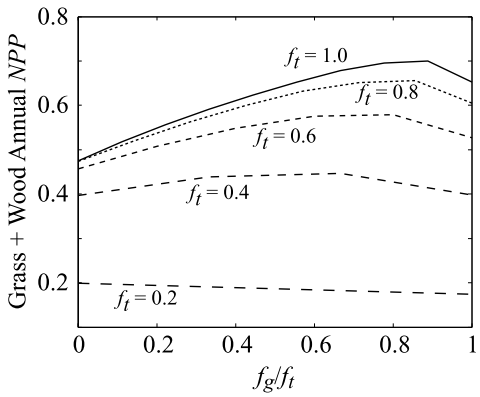

Figure 6. Total grass plus wood annual net primary production versus the grass fraction of total vegetation fractional cover (f_g/f_t) for three states of total vegetation cover (f_t).

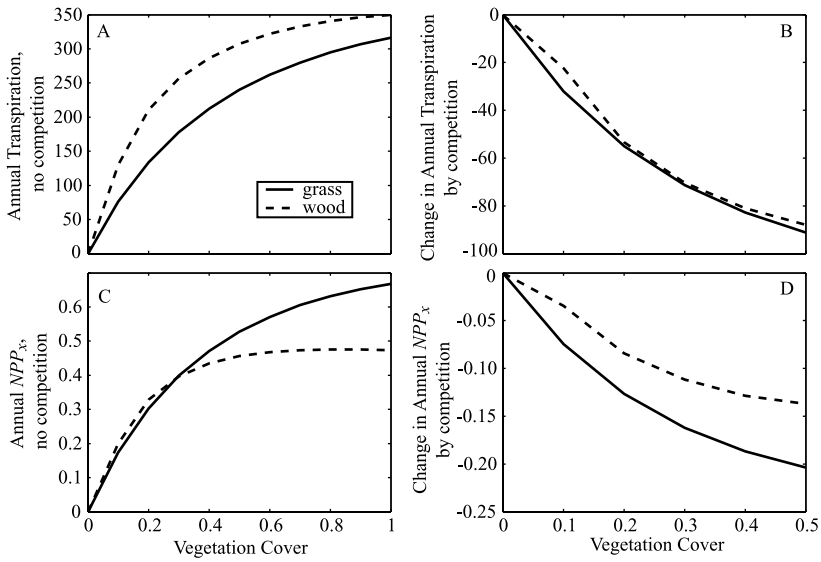

Figure 7. (a) Annual transpiration and (c) production versus vegetation cover in the absence of competition, as well as the change in (b) annual transpiration and (d) production with a competitor vegetation cover of 0.5.

through March) values, as identified from retrospective analysis of the dynamic case (f_g = 0.60, f_w = 0.21). Vegetation dynamics significantly alter both grass and wood transpiration at daily timescales, as evidenced by the wide ranges of their dynamic to static ratios (Figure 8). Linear dependence of transpiration on biomass (meaning $f_x\mathrm{LAI}_x$) is apparent in the scatter when dynamic and static cases have equivalent soil water limitation functions (β_x), with a clearer relationship for grass than wood (Figures 8a and 8b). Grass exhibits a wider range of excursions in the dynamic to static ratio, consistent with larger fluctuations in grass cover compared to that for wood. When grass biomass ($f_g\mathrm{LAI}_g$) is greater for the dynamic case, departure from linear dependence is more pronounced, and this asymmetry suggests that, on average, grass transpiration is lower for the dynamic case (Figure 8a). More importantly, variation in soil water depletion rates and corresponding variation in antecedent soil moisture conditions prior to rain events cause deviation from a 1:1 relationship biased toward a dynamic to static ratio of transpiration equal to one, as soil water limitation offsets the initial departure associated with higher or lower vegetation cover or leaf area. Therefore even at the interstorm timescale, soil water control reduces the effect of vegetation dynamics on transpiration.

[23] Average seasonal trends are shown in Figure 9, represented by the average for each day of year from the 30 simulation years and smoothed with a 30-day moving average. Vegetation dynamics suppress grass transpiration and grass structure relative to the static case in the early wet season (October through January), but elevate them during the late wet season (February through March) through early dry season (Figure 9a). We note that the absolute effect during the dry season is small since transpiration is negligible. Unlike for grass, seasonal trends of wood dynamic to static ratios are out of phase and of smaller magnitude compared to grass ratios (Figure 9b). The dynamic to static ratio for wood transpiration peaks during the dry to wet season transition (December) despite a seasonal low in wood structure indicating that seasonal variation in grass water use is more influential on wood transpiration than are dynamics of the wood vegetation state. Enhanced wood water use in the early wet season and early dry season when grass vegetation is relatively inactive is consistent with the theory of temporal niche separation between grass and

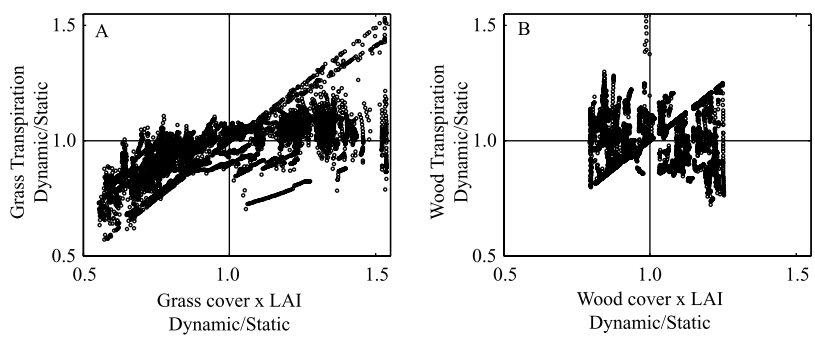

Figure 8. The ratio of dynamic to static daily transpiration versus the ratio of dynamic to static fractional cover times leaf area index ($f_x\mathrm{LAI}_x$) for (a) grass and (b) wood.

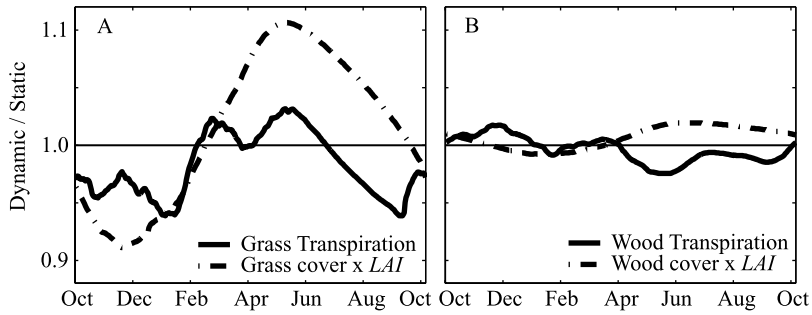

Figure 9. Daily ratio of dynamic to static transpiration and fractional cover times leaf area index (f_xLAI$_x$) averaged for each day of year from the 30 simulation years for (a) grass and (b) wood.

wood [*Scholes and Walker*, 1993], and emphasizes that grass dormancy enhances wood water acquisition. Overall, vegetation dynamics influence daily and seasonal distributions of grass transpiration, but have little effect on wood transpiration except through a mild increase with decreased grass cover.

[24] Figures 10a and 10b illustrate effects of vegetation dynamics on annual vegetation water and carbon fluxes from the 30-year simulations. Vegetation dynamics have almost no effect on annual transpiration or net primary production for grass and wood, evidenced by little deviation from the 1:1 line. In fact, annual rainfall explains most of the variability ($R > 0.85$) in annual vegetation fluxes for both the dynamic and static cases (Figures 10c and 10d). Hence, despite alteration of daily and seasonal distributions of fluxes, at an annual timescale the vegetation dynamics captured in our modeling scheme have little effect on transpiration and production, which are almost exclusively controlled by rainfall for this soil-climate combination.

[25] Dynamics of vegetation cover and composition have been hypothesized as a mechanism for explaining persistence in weather anomalies [*Wang and Eltahir*, 2000; *Zeng and Neelin*, 2000]. Evidence of interannual memory in vegetation production [*Anderson and Inouye*, 2001; *Oesterheld et al.*, 2001; *Wiegand et al.*, 2004] and poor correlation, in some cases, between annual production or vegetation structure and annual rainfall [*Goward and Prince*, 1995; *Oesterheld et al.*, 2001] support this claim. In contrast, *Grist et al.* [1997] showed strong correlation between monthly NDVI and rainfall for the Kalahari, calling into question assertions that lagged vegetation response to climate dynamics, and land cover feedbacks, influence atmospheric persistence at seasonal and greater timescales [e.g., *Goward and Prince*, 1995; *Wang and Eltahir*, 2000]. Our results suggest that vegetation typical

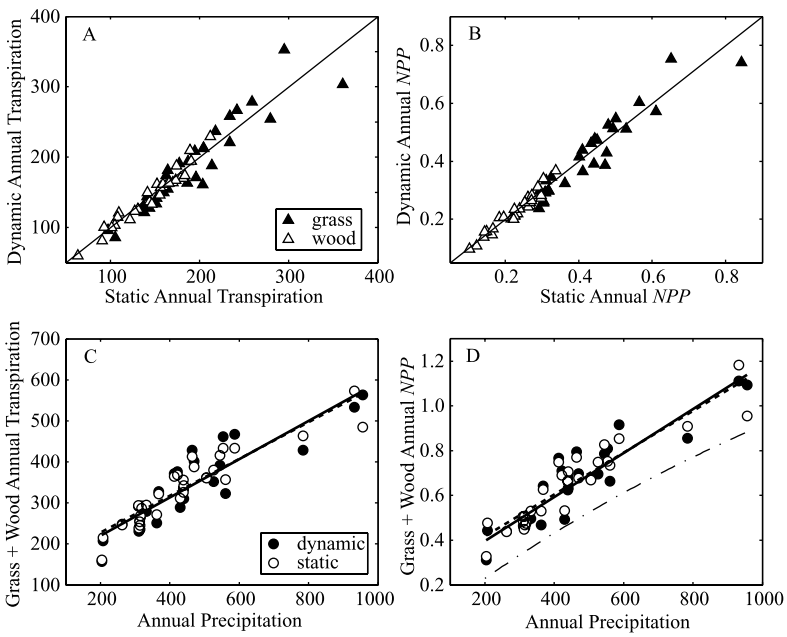

Figure 10. Dynamic versus static annual (a) transpiration and (b) net primary production, as well as total grass plus wood annual (c) transpiration and (d) net primary production versus annual rainfall for the 30 simulation years. The dash-dotted line in Figure 10d indicates twice the aboveground net primary production estimated with the empirically based model of *Huxman et al.* [2004] provided for reference.

of water-limited ecosystems absorbs most of the interannual variability in precipitation and that dynamics of vegetation introduce little energy (memory) into land-atmosphere exchanges of water and carbon at interannual timescales.

[26] Though we can only speculate about how our conclusions would be altered if we were to include disturbance processes, such as vegetation removal by intense fire or grazing, the static simulations can provide insights into the likely effects on water and carbon fluxes. For example, in the extreme case of uncharacteristically low vegetation cover, static simulations show that the sum of annual evaporative fluxes is substantially lower than in a moderately to highly vegetated scenario. Hence leakage may be temporarily increased and total evaporation and production may be temporarily decreased by vegetation removal. Observational studies show that grass can recover completely within one growing season following an intense burn [e.g., *Trollope et al.*, 1996]. Hence a temporary transient of low evapotranspiration and net primary production associated with large bare soil cover may be rapidly dissipated returning to a state where nearly all of annual rainfall is evaporated from the land surface and production is largely controlled by annual rainfall.

[27] While these findings apply broadly to water-limited ecosystems, we should note potential limits to their generalization. In this application, coarse soils with low unsaturated hydraulic conductivity contributed to small leakage and bare soil evaporation fluxes as well as high infiltration rates (near zero runoff), which combined to make nearly all of annual rainfall available to vegetation in years of dry or average wetness in the presence of moderate to full vegetation cover. For low vegetation cover and in years of high rainfall for which soil moisture remains relatively high, leakage and bare soil evaporation assume greater importance in the annual surface water balance and reduce the fraction of annual rainfall available to vegetation. Correspondingly, bare soil evaporation may be prolonged by finer textured soils that could enhance delivery of deep soil moisture to the near surface soil evaporation boundary, potentially causing greater sensitivity of water and carbon fluxes to variation in total vegetation cover.

[28] Our findings suggest that, in drylands, a wide variety of combined grass-wood vegetation states can result in similar annual water and carbon fluxes. In light of these findings it is possible to imagine multiple vegetation states that all yield effectively the same annual water use and even similar productivity, but have vastly different vegetation compositions. This raises an interesting contrast between ecophysiological stability, as described in this study, versus compositional stability. The model may be useful for characterizing grass-wood states and competitive interactions for a range of hydrologic settings that are dictated by various soil-climate combinations. In addition, the model may be useful for quantifying the sensitivity of grass and wood states to possible changes in climate.

4. Conclusions

[29] Our analysis focused on daily to annual timescale responses of water and carbon fluxes to both imposed static and dynamic vegetation states for a range of rainfall conditions typical of arid and semiarid regions. At the daily timescale, transpiration is sensitive to the coincident states of wood and grass fractional covers immediately following wetting events, however the accumulated effect diminishes over the interstorm period with continued soil water depletion. At the seasonal timescale, vegetation dynamics induce seasonal patterns in grass and wood transpiration, however, integrated annual fluxes are insensitive to vegetation dynamics and are almost completely controlled by annual rainfall. Furthermore, we find little sensitivity of annual evapotranspiration to vegetation states except in the wettest conditions when total vegetation cover, particularly wood cover, influences the fraction of annual rainfall lost to leakage. In sum, soil water depletion and corresponding water limitation prevent vegetation dynamics from having an effect on transpiration and evapotranspiration lasting over interstorm to annual timescales despite an initial response immediately following wetting.

[30] In contrast to water fluxes, carbon fluxes are sensitive to the imposed static state of vegetation cover and composition despite water limitation, since respiration depends not only on soil water status but also vegetation biomass. However, natural fluctuations of grass and wood covers as in the dynamic simulations have almost no effect on grass or wood annual production, indicating that vegetation states fluctuate with seasonal to annual variation in water availability with little intraseasonal lag. Therefore annual production influences vegetation cover but vegetation cover has only a minor influence on annual production. In conclusion, our results suggest that for arid and semiarid regions, vegetation cover and rainfall conditions cause the prevailing state to be water-limited such that typical vegetation dynamics are likely to have little effect on annual vegetation water use and corresponding production.

Appendix A: Water Balance Terms

[31] Soil moisture is simulated for two zones, shallow (θ_1, m^3 H_2O m^{-3} soil) and deep (θ_2, m^3 H_2O m^{-3} soil) as by *Scanlon and Albertson* [2003], as

$$\frac{d\theta_1}{dt} = \left[\left(P - I_g - I_w\right) - D - E - T_g - T_{w1}\right] d_1^{-1}, \tag{A1a}$$

$$\frac{d\theta_2}{dt} = \left[D - L - T_{w2}\right] d_2^{-1}, \tag{A1b}$$

where t is time (d), P is precipitation, I_g and I_w are grass and wood interceptions, D is soil water flux, L is leakage, E is bare soil evaporation rate, T_g, T_{w1}, and T_{w2} are grass and wood transpiration rates, all having units of mm d^{-1} on a ground area basis and described further below, and d_1 and d_2 are shallow and deep soil zone thicknesses. Parameters and constants are defined in Table 1. With equation (1), we adopt an implicit assumption common to many soil water balance models [e.g., *Paruelo and Sala*, 1995; *Walker and Langridge*, 1996; *Reynolds et al.*, 2000] that grass and wood access a common shallow soil moisture pool subject to bare soil evaporation losses, while wood has exclusive access to a deeper soil water reservoir, as illustrated in Figure 1.

[32] Interception is modeled as

$$I_x = \min(Pf_x, I_{x\max} f_x - J_x), \tag{A2}$$

where $I_{x\max}$ is the maximum potential interception (mm d^{-1}), and f_x is fractional cover (see B5). The subscript x

refers to grass (g), wood (w), or bare soil (b) as appropriate. Interception storage (J_x, mm) is subject to direct evaporation, as

$$\frac{dJ_x}{dt} = I_x - \min(\mathrm{PET}_x f_x, J_x), \tag{A3}$$

reducing the energy available for transpiration (see equations (A6a), (A6b), and (A6c)). Vertical soil water flux between the root zone compartments is modeled with Darcy's law for unsaturated flow, as

$$D = -K_1\left(\frac{\psi_2 - \psi_1}{(0.5d_2 + d_1) - 0.5d_1} - 1\right), \tag{A4}$$

where K_1 is the shallow zone unsaturated hydraulic conductivity (mm d^{-1}), ψ_1 and ψ_2 are soil water potentials (mm H_2O) in the shallow and deep zones. Assuming a unit head gradient, L is equivalent to the deep zone unsaturated hydraulic conductivity (K_2, mm d^{-1}). K_1 and K_2 are after *Clapp and Hornberger* [1978]. Surface runoff and ponding are not considered owing to the high infiltration capacity of the sandy Kalahari soils, as assumed by *Scanlon and Albertson* [2003]. If infiltration, equivalent to P-I_g-I_w, exceeds the upper soil zone storage capacity, defined by $d_1(n\text{-}\theta_1)$, where n is porosity (m^3 void m^{-3} soil), excess water is routed directly through to the lower soil zone. Bare soil evaporation rate follows

$$E = \mathrm{PET}_b f_b \beta_b(\theta_1), \tag{A5}$$

where $\beta_b(\theta_1)$ is the bare soil water limitation function as described in equation A9.

[33] Daily transpiration rates for grass (T_g, mm d^{-1}), wood from θ_1 (T_{w1}, mm d^{-1}), and wood from θ_2 (T_{w2}, mm d^{-1}) are modeled as

$$T_g = \left(\mathrm{PET}_g f_g - \min\left(\mathrm{PET}_g f_g, J_g\right)\right)\min\left(\mathrm{LAI}_g, 1\right)\beta_g(\theta_1), \tag{A6a}$$

$$\mathrm{T}_{w1} = (\mathrm{PET}_w f_w - \min(\mathrm{PET}_w f_w, J_w))\min(\mathrm{LAI}_w, 1)\beta_w(\theta_1)\varepsilon_1, \tag{A6b}$$

$$T_{w2} = (\mathrm{PET}_w f_w - \min(\mathrm{PET}_w f_w, J_w))\min(\mathrm{LAI}_w, 1)\beta_w(\theta_2)(1 - \varepsilon_1), \tag{A6c}$$

and $T_w = T_{w1} + T_{w2}$, where LAI_x is leaf area index (see (B6)), $\beta_b(\theta_1)$ is the bare soil water limitation function (see (A9)), and ε_1 is the fraction of wood roots in the upper soil zone. Potential evapotranspiration rate (PET_x, mm d^{-1}) is estimated with the *Priestley and Taylor* [1972] formulation, as

$$\mathrm{PET}_x = \left[\kappa(Rn_x(1 - Cg))\frac{\Delta}{\Delta + \gamma}\right]\frac{\tau}{\rho_v V}, \tag{A7}$$

where κ is 1.26, Δ is the slope of the saturation vapor pressure curve (kPa $°C^{-1}$), γ is the psychrometric constant (0.067 kPa $°C^{-1}$), ρ_v is the density of water, τ is the duration of daylight per day (s d^{-1}), V is the latent heat of vaporization (J kg^{-1} H_2O), Cg (0.3) is a soil heat flux coefficient as in the work by *Lhomme and Monteny* [2000], and in agreement with observations reported by *Williams and Albertson* [2004], and Rn_x is obtained as

$$Rn_x = Rsw \downarrow (1 - \nu_x) + Rlwn \tag{A8}$$

where υ_x is albedo [*Campbell and Norman*, 1998]. The soil water limitation functions are of the form

$$\beta_x(\theta_y) = \begin{cases} 1 & \text{for } \theta_y \geq \theta_{xcr} \\ \left[\dfrac{\theta_y - \theta_{xlim}}{\theta_{xcr} - \theta_{xlim}}\right]^m & \text{for } \theta_{xlim} < \theta_y < \theta_{xcr}, \\ 0 & \text{for } \theta_y \leq \theta_{xlim} \end{cases} \tag{A9}$$

where subscript $y = 1$ or 2, and $m = 1$ for vegetation and 2 for soil, β_w is obtained from $\beta_w(\theta_1)\varepsilon_1 + \beta_w(\theta_2)(1 - \varepsilon_1)$, and θ_{xlim} is a limit point for E or T_x. *Williams and Albertson* [2004] reported good approximation of observed ratios of evapotranspiration to PET by the soil moisture limitation function.

Appendix B: Carbon Balance Terms

[34] Dynamics of vegetation biomass are modeled with a conventional mass balance [*Chen et al.*, 1996; *LoSeen et al.*, 1997; *Calvet et al.*, 1998], as

$$\frac{dX_l}{dt} = (T_x \mathrm{WUE}_x \rho_v \omega - \mathrm{Re}_x)\Phi_{xl} - \Gamma_{xl} X_l + \eta_x, \tag{B1a}$$

$$\frac{dX_s}{dt} = (T_x \mathrm{WUE}_x \rho_v \omega - \mathrm{Re}_x)(1 - \Phi_{xl}) - \Gamma_{xs} X_s - \eta_x, \tag{B1b}$$

where X_l and X_s refer to grass (G, kg grass DM m^{-2} ground) or wood (W, kg wood DM m^{-2} ground) biomass in the leaf (subscript l) and structural (subscript s) pools, respectively, Φ_{xl} is fractional leaf allocation, Γ_{xl} and Γ_{xs} are natural decay factors, η_x is a leaf flush factor, each described further below, and ρ_v and ω clear the units. A simple coupling of water and carbon fluxes with a water use efficiency (WUE_x, kg CO_2 kg^{-1} H_2O) is supported by *Williams and Albertson* [2004], reporting a linear relationship between ET and F_c over a wide range of soil moisture from observations at the Ghanzi savanna. Thus we adopt

$$\mathrm{WUE}_x = \frac{g_c(1 - \alpha_x)C_a}{g_v(q^* - q)}\mu, \tag{B2}$$

where g_c and g_v are air diffusivities of CO_2 and H_2O vapor (m^2 s^{-1}), C_a is ambient CO_2 concentration (μmol CO_2 mol^{-1} air), q^* is saturated specific humidity of air (kg H_2O kg^{-1} air), μ clears the units (1.5×10^{-6} g CO_2 g^{-1} air). Nonleaf plant respiration rate (Re_x, kg DM m^{-2} d^{-1}) is estimated with soil moisture, temperature, and biomass dependence based on the maintenance respiration model outlined by *Sitch et al.* [2003], which includes a modified Arrhenius equation [*Lloyd and Taylor*, 1994] following the approach of *Ryan* [1991]. Daily net primary production (NPP_x, kg DM m^{-2}) is

$$\mathrm{NPP}_x = T_x \mathrm{WUE}_x \rho_v \omega - \mathrm{Re}_x. \tag{B3}$$

[35] Fractional allocation of daily production to leaves (Φ_{xl}) follows

$$\Phi_{xl} = 1 - \frac{\mathrm{LAI}_x}{\mathrm{LAI}_{x\max}}, \tag{B4}$$

where $\mathrm{LAI}_{x\max}$ is the maximum LAI_x (m^2 leaf m^{-2} vegetation). This form was adopted because production tends to be allocated to leaves in the early growing season and roots and stems in the late growing season [*Scholes and Walker*, 1993; *Larcher*, 1995]. Decay factors for structural biomass (Γ_{gs}, Γ_{ws}) are assumed to be constants, as is typical in vegetation dynamics models [*Walker et al.*, 1981; *LoSeen et al.*, 1997; *Verhoef and Allen*, 2000; *Anderies et al.*, 2002; *Sitch et al.*, 2003; *van Langevelde et al.*, 2003]. Leaf decay factors (Γ_{gl}, Γ_{wl}, d^{-1}) are also typically modeled as constant except after extended stress (ξ_x, see B8) [*Cayrol et al.*, 2000; *Sitch et al.*, 2003; *Jolly and Running*, 2004], modeled here as a doubling of leaf decay factors if $\langle \xi_x \rangle_{30}$ exceeds ξ_{*x}, where $\langle\ \rangle$ is the time average operator and the subscript identifies the number of previous, consecutive days included in the time average. Leaf flush is similar to that of *Lo Seen et al.* [1997] and *Jolly and Running* [2004], with a shift of biomass from the structural to leaf pool (η_x) at the beginning of the growing season, between 1 October and 31 December for our study region [*Jolly and Running*, 2004], where η_x is $\frac{\Lambda f_x \mathrm{LAI}_{x\max}}{\mathrm{SLA}x}$ and Λ is a leaf flush factor (0.05 d^{-1}), if $\beta_x > \beta_{*x}$ up to a total of 25% of $f_x\mathrm{LAI}_{x\max}$ annually, since only first tissues are produced by stored carbohydrate [*Scholes and Walker*, 1993].

[36] Vegetation fractional cover (f_x, m^2 vegetation cover m^{-2} ground) is obtained as

$$f_x = \frac{X_s}{X_{s\max}}, \tag{B5}$$

where $X_{s\max}$ (kg plant dry matter m^{-2} ground) represents the maximum structural biomass that could occupy a unit of ground area similar to *Eagleson and Segarra* [1985] and *Anderies et al.* [2002]. To ensure that $f_w + f_g + f_b$ does not exceed 1, total fractional cover is partitioned with priority to wood, assuming that grass is inferior to wood in competition for light [*Sitch et al.*, 2003], while $f_b = 1 - f_w - f_g$. Leaf area index within vegetated patches is modeled as

$$\mathrm{LAI}_x = X_l \mathrm{SLA}_x, \tag{B6}$$

where SLA_x is the specific leaf area (m^2 leaf kg^{-1} leaf DM). Figure 1 illustrates that the model calculates leaf area within vegetated patches, which is distributed to a ground area basis by its product with fractional cover, yielding a ground area based leaf area (LAI_{rx}, m^2 leaf m^{-2} ground). Hence vegetation can occupy landscape space (fractional cover) even without supporting active leaf area. For comparison to LAI derived from NDVI, LAI_{rx} is also scaled by vegetation water stress, similar to *Sellers et al.* [1996], because near infrared reflectance is strongly influenced by wilting and plant water content [*Tucker et al.*, 1993; *Roberts et al.*, 1997; *Zarco-Tejada et al.*, 2003a, 2003b], represented as

$$\mathrm{LAI}_{rx} = \mathrm{LAI}_x f_x \left(1 - \langle \xi_x \rangle_{10}\right). \tag{B7}$$

We adopt the vegetation water stress function [*Laio et al.*, 2001]

$$\xi_x(\theta_y) = \begin{cases} 0 & \text{for } \theta_y \geq \theta_{xcr} \\ \left[\dfrac{\theta_{xcr} - \theta_y}{\theta_{xcr} - \theta_{xlim}}\right]^2 & \text{for } \theta_{xlim} < \theta_y < \theta_{xcr}, \\ 1 & \text{for } \theta_y \leq \theta_{xlim} \end{cases} \tag{B8}$$

and ξ_w is obtained from $\xi_w(\theta_1)\varepsilon_1 + \xi_w(\theta_2)(1 - \varepsilon_1)$.

Appendix C: Model Input Data

[37] The model is forced by a set of daily atmospheric conditions. Since our study period exceeds the length of local records, we generated synthetic time series of near surface atmospheric conditions. The stochastic weather generator (WGEN), developed by *Richardson* [1981], was parameterized for the Ghanzi site enabling the generation of synthetic time series of average daytime near surface weather conditions. The wet (rainy) or dry status for each day was dictated by a 30-year data set of daily rainfall (Eaton, unpublished data, 2002). To parameterize WGEN for the Ghanzi site, we obtained data of daily rainfall, average daytime air temperature (φ, °C), air specific humidity (q, kg H_2O kg^{-1} air), average daytime incoming shortwave radiation (*Rsw* ↓, W m^{-2}), and average daytime net (incoming minus outgoing) longwave radiation (*Rlwn*, W m^{-2}) for 1 January 1948 to 31 December 2002 for the 2.5° × 2.5° grid cell encompassing Ghanzi, Botswana, from the National Centers for Environmental Prediction Reanalysis Project (Reanalysis Project data made available online by National Oceanic and Atmospheric Administration Climate Diagnostics Center, http://www.cdc.noaa.gov/). Recognizing the limitations of coarse-scale conditions, we used a linear statistical downscaling [*Kim et al.*, 1984; *Semenov and Barrow*, 1997] of mean daily Reanalysis data for φ and q based on fits to daily observations taken during 1995 to 2000 at the Ghanzi, Botswana, weather station [*GHCN/GSOD*, 2003]. We adjusted the 24-hour averaged φ and *Rsw* ↓ to represent climatic conditions averaged over seasonally variable day lengths. Monthly statistics of means, standard deviations, and serial and cross correlations were obtained from the daytime data, and used to generate daily φ, q, *Rsw* ↓, and *Rlwn* with the multivariate normal procedure, preserving their serial and cross correlations [*Richardson*, 1981; *Richardson and Wright*, 1984].

[38] **Acknowledgments.** The material is based upon work supported by the National Science Foundation under grant 0243598 and was also supported by the Office of Science (BER), U.S. Department of Energy, Cooperative Agreement DE-FCO3-90ER61010. The authors thank Howard Epstein at the University of Virginia for assistance with model development. We thank Kelly Caylor for his valuable comments.

References

Aguiar, M. R., J. M. Paruelo, O. E. Sala, and W. K. Lauenroth (1996), Ecosystem responses to changes in plant functional type composition: An example from the Patagonian steppe, *J. Veg. Sci.*, *7*, 381–390.

Anderies, J. M., M. A. Janssen, and B. H. Walker (2002), Grazing management, resilience, and the dynamics of a fire-driven rangeland system, *Ecosystems*, *5*, 23–44.

Anderson, J. E., and R. S. Inouye (2001), Landscape-scale changes in plant species abundance and biodiversity of a sagebrush steppe over 45 years, *Ecol. Monogr.*, *71*, 531–556.

Ansley, R. J., B. A. Kramp, and D. L. Jones (2003), Converting mesquite thickets to savanna through foliage modification with clopyralid, *J. Range Manage.*, *56*, 72–80.

Atjay, G. L., P. Ketner, and P. Duvigneaud (1979), Terrestrial primary production and phytomass, in *The Global Carbon Cycle*, edited by B. Bolin et al., pp. 129–181, John Wiley, Hoboken, N. J.

Baillieul, T. A. (1975), A reconnaissance survey of the cover sands in the Republic of Botswana, *J. Sediment. Petrol.*, *45*, 494–503.

Baldocchi, D. D., L. K. Xu, and N. Kiang (2004), How plant functional-type, weather, seasonal drought, and soil physical properties alter water and energy fluxes of an oak-grass savanna and an annual grassland, *Agric. For. Meteorol.*, *123*, 13–39.

Bellot, J., A. Bonet, J. R. Sanchez, and E. Chirino (2001), Likely effects of land use changes on the runoff and aquifer recharge in a semiarid landscape using a hydrological model, *Landscape Urban Plann.*, *55*, 41–53.

Betts, R. A., P. M. Cox, S. E. Lee, and F. I. Woodward (1997), Contrasting physiological and structural vegetation feedbacks in climate change simulations, *Nature*, *387*, 796–799.

Bonan, G. B. (1995), Land atmosphere interactions for climate system models—Coupling biophysical, biogeochemical, and ecosystem dynamical processes, *Remote Sens. Environ.*, *51*, 57–73.

Bonan, G. B., S. Levis, S. Sitch, M. Vertenstein, and K. W. Oleson (2003), A dynamic global vegetation model for use with climate models: Concepts and description of simulated vegetation dynamics, *Global Change Biol.*, *9*, 1543–1566.

Brutsaert, W. H. (1982), *Evaporation Into the Atmosphere: Theory, History, and Applications*, Springer, New York.

Calvet, J.-C., J. Noilhan, J.-L. Roujean, P. Bessemoulin, M. Cabelguenne, A. Olioso, and J.-P. Wigneron (1998), An interactive vegetation SVAT model tested against data from six contrasting sites, *Agric. For. Meteorol.*, *92*, 73–95.

Campbell, G. S., and J. M. Norman (1998), *An Introduction to Environmental Biophysics*, 2nd ed., Springer, New York.

Caylor, K. K., H. H. Shugart, P. R. Dowty, and T. M. Smith (2003), Tree spacing along the Kalahari transect in southern Africa, *J. Arid Environ.*, *54*, 281–296.

Cayrol, P., A. Chehbouni, L. Kergoat, G. Dedieu, P. Mordelet, and Y. Nouvellon (2000), Grassland modeling and monitoring with SPOT-4 VEGETATION instrument during the 1997–1999 SALSA experiment, *Agric. For. Meteorol.*, *105*, 91–115.

Charney, J. G. (1975), The dynamics of deserts and droughts, *Q. J. R. Meteorol. Soc.*, *101*, 193–202.

Chen, D. X., H. W. Hunt, and J. A. Morgan (1996), Responses of a C-3 and C-4 perennial grass to CO_2 enrichment and climate change: Comparison between model predictions and experimental data, *Ecol. Modell.*, *87*, 11–27.

Clapp, R. B., and G. M. Hornberger (1978), Empirical equations for some soil hydraulic-properties, *Water Resour. Res.*, *14*, 601–604.

de Vries, J. J., E. T. Selaolo, and H. E. Beekman (2000), Groundwater recharge in the Kalahari, with reference to paleo-hydrologic conditions, *J. Hydrol.*, *238*, 110–123.

Dickinson, R. E., and A. Henderson-Sellers (1988), Modeling tropical deforestation—A study of GCM land surface parametrizations, *Q. J. R. Meteorol. Soc.*, *114*, 439–462.

Eagleson, P. S. (1978a), Climate, soil, and vegetation: 1. Introduction to water-balance dynamics, *Water Resour. Res.*, *14*, 705–712.

Eagleson, P. S. (1978b), Climate, soil, and vegetation: 6. Dynamics of annual water-balance, *Water Resour. Res.*, *14*, 749–764.

Eagleson, P. S., and R. I. Segarra (1985), Water-limited equilibrium of savanna vegetation systems, *Water Resour. Res.*, *21*, 1483–1493.

Eamus, D. (1999), Ecophysiological traits of deciduous and evergreen woody species in the seasonally dry tropics, *Trends Ecol. Evol.*, *4*, 1–6.

Ehleringer, J. R., and R. K. Monson (1993), Evolutionary and ecological aspects of photosynthetic pathway variation, *Annu. Rev. Ecol. Syst.*, *24*, 411–439.

Foley, J. A., I. C. Prentice, N. Ramankutty, S. Levis, D. Pollard, S. Sitch, and A. Haxeltine (1996), An integrated biosphere model of land surface processes, terrestrial carbon balance, and vegetation dynamics, *Global Biogeochem. Cycles*, *10*, 603–628.

Foley, J. A., S. Levis, M. H. Costa, W. Cramer, and D. Pollard (2000), Incorporating dynamic vegetation cover within global climate models, *Ecol. Appl.*, *10*, 1620–1632.

Gaze, S. R., J. Brouwer, L. P. Simmonds, and J. Bromley (1998), Dry season water use patterns under *Guiera senegalensis* L. shrubs in a tropical savanna, *J. Arid Environ.*, *40*, 53–67.

GHCN/GSOD (2003), Global Historical and Climatological Network, and Global Summary of the Day, data made available online by National Oceanic and Atmospheric Administration National Climate Data Center.

Golluscio, R. A., O. E. Sala, and W. K. Lauenroth (1998), Differential use of large summer rainfall events by shrubs and grasses: A manipulative experiment in the Patagonian steppe, *Oecologia*, *115*, 17–25.

Goward, S. N., and S. D. Prince (1995), Transient effects of climate on vegetation dynamics: Satellite observations, *J. Biogeogr.*, *22*, 549–564.

Grist, J., S. E. Nicholson, and A. Mpolokang (1997), On the use of NDVI for estimating rainfall fields in the Kalahari of Botswana, *J. Arid Environ.*, *35*, 195–214.

Guillevic, P., R. D. Koster, M. J. Suarez, L. Bounoua, G. J. Collatz, S. O. Los, and S. P. P. Mahanama (2002), Influence of the interannual variability of vegetation on the surface energy balance—A global sensitivity study, *J. Hydrometeorol.*, *3*, 617–629.

House, J. I., S. Archer, D. D. Breshears, and R. J. Scholes (2003), Conundrums in mixed woody-herbaceous plant systems, *J. Biogeogr.*, *30*, 1763–1777.

Hutley, L. B., A. P. O'Grady, and D. Eamus (2000), Evapotranspiration from eucalypt open-forest savanna of northern Australia, *Funct. Ecol.*, *14*, 183–194.

Hutley, L. B., A. P. O'Grady, and D. Eamus (2001), Monsoonal influences on evapotranspiration of savanna vegetation of northern Australia, *Oecologia*, *126*, 434–443.

Huxman, T. E., et al. (2004), Convergence across biomes to a common rain-use efficiency, *Nature*, *429*, 651–654.

Jackson, R. B., O. E. Sala, J. M. Paruelo, and H. A. Mooney (1998), Ecosystem water fluxes for two grasslands in elevated CO_2: A modeling analysis, *Oecologia*, *113*, 537–546.

Joffre, R., and S. Rambal (1993), How tree cover influences the water-balance of Mediterranean rangelands, *Ecology*, *74*, 570–582.

Jolly, W. M., and S. W. Running (2004), Effects of precipitation and soil water potential on drought deciduous phenology in the Kalahari, *Global Change Biol.*, *10*, 303–308.

Kabat, P., A. J. Dolman, and J. A. Elbers (1997), Evaporation, sensible heat and canopy conductance of fallow savannah and patterned woodland in the Sahel, *J. Hydrol.*, *189*, 494–515.

Kim, J. W., J. T. Chang, N. L. Baker, D. S. Wilks, and W. L. Gates (1984), The statistical problem of climate inversion—Determination of the relationship between local and large-scale climate, *Mon. Weather Rev.*, *112*, 2069–2077.

Laio, F., A. Porporato, L. Ridolfi, and I. Rodriguez-Iturbe (2001), Plants in water-controlled ecosystems: Active role in hydrologic processes and response to water stress—II. Probabilistic soil moisture dynamics, *Adv. Water Resour.*, *24*, 707–723.

Larcher, W. (1995), *Physiological Plant Ecology*, 3rd ed., Springer, New York.

Lhomme, J. P., and B. Monteny (2000), Theoretical relationship between stomatal resistance and surface temperatures in sparse vegetation, *Agric. For. Meteorol.*, *104*, 119–131.

Lloyd, J., and J. A. Taylor (1994), On the temperature-dependence of soil respiration, *Funct. Ecol.*, *8*, 315–323.

LoSeen, D., A. Chehbouni, E. Njoku, S. Saatchi, E. Mougin, and G. Monteny (1997), An approach to couple vegetation functioning and soil-vegetation-atmosphere-transfer models for semiarid grasslands during the HAPEX-Sahel experiment, *Agric. For. Meteorol.*, *83*, 49–74.

Midgley, G. F., J. N. Aranibar, K. B. Mantlana, and S. Macko (2004), Photosynthetic and gas exchange characteristics of dominant woody plants on a moisture gradient in an African savanna, *Global Change Biol.*, *10*, 309–317.

Myneni, R. B., R. R. Nemani, and S. W. Running (1997), Algorithm for the estimation of global land cover, LAI and FPAR based on radiative transfer models, *IEEE Trans. Geosci. Remote Sens.*, *35*, 1380–1393.

Neilson, R. P., and D. Marks (1994), A global perspective of regional vegetation and hydrologic sensitivities from climatic-change, *J. Veg. Sci.*, *5*, 715–730.

Noy-Meir, I. (1973), Desert ecosystems: Environment and producers, *Annu. Rev. Ecol. Syst.*, *4*, 25–44.

Oesterheld, M., J. Loreti, M. Semmartin, and O. E. Sala (2001), Inter-annual variation in primary production of a semiarid grassland related to previous-year production, *J. Veg. Sci.*, *12*, 137–142.

Paruelo, J. M., and O. E. Sala (1995), Water losses in the Patagonian steppe—A modeling approach, *Ecology*, *76*, 510–520.

Pearcy, R. W., and J. Ehleringer (1984), Comparative ecophysiology of C-3 and C-4 plants, *Plant Cell Environ.*, *7*, 1–13.

Priestley, C. H. B., and R. J. Taylor (1972), On the assessment of surface heat flux and evaporation using large-scale parameters, *Mon. Weather Rev.*, *100*, 81–92.

Reynolds, J. F., P. R. Kemp, and J. D. Tenhunen (2000), Effects of long-term rainfall variability on evapotranspiration and soil water distribution in the Chihuahuan Desert: A modeling analysis, *Plant Ecol.*, *150*, 145–159.

Richardson, C. W. (1981), Stochastic simulation of daily precipitation, temperature, and solar radiation, *Water Resour. Res.*, *17*, 182–190.

Richardson, C. W., and G. C. Wright (1984), WGEN: A model for generating daily weather variables, *ARS-8*, 83 pp., Agric. Res. Serv., U.S. Dep. of Agric., Washington, D. C.

Roberts, D. A., R. O. Green, and J. B. Adams (1997), Temporal and spatial patterns in vegetation and atmospheric properties from AVIRIS, *Remote Sens. Environ.*, *62*, 223–240.

Rodriguez-Iturbe, I., P. D'Odorico, A. Porporato, and L. Ridolfi (1999a), On the spatial and temporal links between vegetation, climate, and soil moisture, *Water Resour. Res.*, *35*, 3709–3722.

Rodriguez-Iturbe, I., P. D'Odorico, A. Porporato, and L. Ridolfi (1999b), Tree-grass coexistence in savannas: The role of spatial dynamics and climate fluctuations, *Geophys. Res. Lett.*, *26*, 247–250.

Rodriguez-Iturbe, I., A. Porporato, L. Ridolfi, V. Isham, and D. R. Cox (1999c), Probabilistic modelling of water balance at a point: The role of climate, soil and vegetation, *Proc. R. Soc. London, Ser. A*, *455*, 3789–3805.

Ryan, M. G. (1991), A simple method for estimating gross carbon budgets for vegetation in forest ecosystems, *Tree Physiol.*, *9*, 255–266.

Sakai, R. K., D. R. Fitzjarrald, O. L. L. Moraes, R. M. Staebler, O. C. Acevedo, M. J. Czikowsky, R. Da Silva, E. Brait, and V. Miranda (2004), Land-use change effects on local energy, water, and carbon balances in an Amazonian agricultural field, *Global Change Biol.*, *10*, 895–907.

Sala, O. E., and W. K. Lauenroth (1982), Small rainfall events—An ecological role in semi-arid regions, *Oecologia*, *53*, 301–304.

Sala, O. E., W. K. Lauenroth, and W. J. Parton (1992), Long-term soil-water dynamics in the shortgrass steppe, *Ecology*, *73*, 1175–1181.

San Jose, J. J., R. Bracho, and N. Nikonova (1998), Comparison of water transfer as a component of the energy balance in a cultivated grass (*Brachiaria decumbens* Stapf.) field and a savanna during the wet season of the Orinoco Llanos, *Agric. For. Meteorol.*, *90*, 65–79.

Santos, A. J. B., G. Silva, H. S. Miranda, A. C. Miranda, and J. Lloyd (2003), Effects of fire on surface carbon, energy and water vapour fluxes over campo sujo savanna in central Brazil, *Funct. Ecol.*, *17*, 711–719.

Scanlon, T. M., and J. D. Albertson (2003), Inferred controls on tree/grass composition in a savanna ecosystem: Combining 16-year normalized difference vegetation index data with a dynamic soil moisture model, *Water Resour. Res.*, *39*(8), 1224, doi:10.1029/2002WR001881.

Schenk, H. J., and R. B. Jackson (2002), Rooting depths, lateral root spreads and below-ground/above-ground allometries of plants in water-limited ecosystems, *J. Ecol.*, *90*, 480–494.

Scholes, R. J., and S. R. Archer (1997), Tree-grass interactions in savannas, *Annu. Rev. Ecol. Syst.*, *28*, 517–544.

Scholes, R. J., and B. H. Walker (1993), *An African Savanna: Synthesis of the Nylsvley Study*, Cambridge Univ. Press, New York.

Scholes, R. J., P. R. Dowty, K. Caylor, D. A. B. Parsons, P. G. H. Frost, and H. H. Shugart (2002), Trends in savanna structure and composition along an aridity gradient in the Kalahari, *J. Veg. Sci.*, *13*, 419–428.

Sellers, P. J., S. O. Los, C. J. Tucker, C. O. Justice, D. A. Dazlich, G. J. Collatz, and D. A. Randall (1996), A revised land surface parameterization (SiB2) for atmospheric GCMs. 2. The generation of global fields of terrestrial biophysical parameters from satellite data, *J. Clim.*, *9*, 706–737.

Semenov, M. A., and E. M. Barrow (1997), Use of a stochastic weather generator in the development of climate change scenarios, *Clim. Change*, *35*, 397–414.

Sitch, S., et al. (2003), Evaluation of ecosystem dynamics, plant geography and terrestrial carbon cycling in the LPJ dynamic global vegetation model, *Global Change Biol.*, *9*, 161–185.

Smith, T. M., H. H. Shugart, and F. I. Woodward (1997), *Plant Functional Types: Their Relevance to Ecosystem Properties and Global Change*, Cambridge Univ. Press, New York.

Soloman, A. M., and H. H. Shugart (1993), *Vegetation Dynamics and Global Change*, CRC Press, Boca Raton, Fla.

Trollope, W. S. W., L. A. Trollope, A. F. L. Potgieter, and N. Zambatis (1996), SAFARI-92 characterization of biomass and fire behavior in the small experimental burns in the Kruger National Park, *J. Geophys. Res.*, *101*, 23,531–23,539.

Tucker, G. F., J. P. Lassoie, and T. J. Fahey (1993), Crown architecture of stand-grown sugar maple (*Acer saccharum* Marsh) in the Adirondack Mountains, *Tree Physiol.*, *13*, 297–310.

van Langevelde, F., et al. (2003), Effects of fire and herbivory on the stability of savanna ecosystems, *Ecology*, *84*, 337–350.

Veenendaal, E. M., O. Kolle, and J. Lloyd (2004), Seasonal variation in energy fluxes and carbon dioxide exchange for a broad-leaved semi-arid savanna (Mopane woodland) in Southern Africa, *Global Change Biol.*, *10*, 318–328.

Verhoef, A., and S. J. Allen (2000), A SVAT scheme describing energy and CO_2 fluxes for multi-component vegetation: Calibration and test for a Sahelian savannah, *Ecol. Modell.*, *127*, 245–267.

Verhoef, A., S. J. Allen, H. A. R. DeBruin, C. M. J. Jacobs, and B. G. Heusinkveld (1996), Fluxes of carbon dioxide and water vapour from a Sahelian savanna, *Agric. For. Meteorol.*, *80*, 231–248.

von Randow, C., et al. (2004), Comparative measurements and seasonal variations in energy and carbon exchange over forest and pasture in south west Amazonia, , *78*, 5–26.

Walker, B. H., and J. L. Langridge (1996), Modelling plant and soil water dynamics in semi-arid ecosystems with limited site data, *Ecol. Modell.*, *87*, 153–167.

Walker, B. H., D. Ludwig, C. S. Holling, and R. M. Peterman (1981), Stability of semi-arid savanna grazing systems, *J. Ecol.*, *69*, 473–498.

Walter, H. (1971), *Ecology of Tropical and Subtropical Vegetation*, Oliver and Boyd, Edinburgh, U. K.

Wang, G. L., and E. A. B. Eltahir (2000), Role of vegetation dynamics in enhancing the low-frequency variability of the Sahel rainfall, *Water Resour. Res.*, *36*, 1013–1021.

Wiegand, T., H. A. Snyman, K. Kellner, and J. M. Paruelo (2004), Do grasslands have a memory: Modeling phytomass production of a semi-arid South African grassland, *Ecosystems*, *7*, 243–258.

Wilcox, B. P. (2002), Shrub control and streamflow on rangelands: A process based viewpoint, *J. Range Manage.*, *55*, 318–326.

Williams, C. A., and J. D. Albertson (2004), Soil moisture controls on canopy-scale water and carbon fluxes in an African savanna, *Water Resour. Res.*, *40*, W09302, doi:10.1029/2004WR003208.

Yong-Quiang, L., Y. Du-Zheng, and J. Jin-Jun (1992), Influence of soil moisture and vegetation on climate (I): Theoretical analysis to persistence of short-term climate anomalies, *Sci. China, Ser. B*, *35*, 1485–1493.

Zarco-Tejada, P. J., J. C. Pushnik, S. Dobrowski, and S. L. Ustin (2003a), Steady-state chlorophyll a fluorescence detection from canopy derivative reflectance and double-peak red-edge effects, *Remote Sens. Environ.*, *84*, 283–294.

Zarco-Tejada, P. J., C. A. Rueda, and S. L. Ustin (2003b), Water content estimation in vegetation with MODIS reflectance data and model inversion methods, *Remote Sens. Environ.*, *85*, 109–124.

Zeng, N., and J. D. Neelin (2000), The role of vegetation-climate interaction and interannual variability in shaping the African savanna, *J. Clim.*, *13*, 2665–2670.

J. D. Albertson, Department of Civil and Environmental Engineering, Duke University, Durham, NC 27708-0287, USA. (john.albertson@duke.edu)

C. A. Williams, Natural Resource Ecology Laboratory, Colorado State University, Fort Collins, CO 80523-1499, USA. (caw@nrel.colostate.edu)